Increasing oil temperature and the optimum mass flow rate and weather conditions over the year

Karim ElFeky[1], Abdalla Hanafi[2], W. Abbas[1], Mahmoud AlKady[3]

[1] **Basic and Applied Sciences Department, College of Engineering and Technology, Arab Academy for Science and Technology, Cairo, Egypt.**
[2] **Mechanical Power Engineering Department, Faculty of Engineering, Cairo University, Cairo, Egypt.**
[3] **Mechanical Power Engineering Department, Faculty of Engineering, Al Azhar University, Cairo, Egypt.**

Abstract

Large-scale renewable energy sources with tremendous potential include concentrated solar power, which is currently attracting attention due to its use and room for growth. Due to their higher efficiency when compared to photovoltaic, parabolic trough solar collectors (PTSCs) in particular are becoming more and more popular. This work aims to assess the performance of a planned 24-m-long PTSC model in a $10m^3$/day solar MED water desalination plant with a $2.2m^3$ storage tank. Oil served as the working fluid in a glass heat-collection element. Based on seasonal data for average intake and outflow temperatures and surface temperatures for Cairo's climatic conditions, the suggested model's authentication is supported.

Keywords: optimum mass flow; renewable energy; parabolic trough solar collectors.

1 Introduction

The sun can be visualized as a 1.39 x 109 m-diameter sphere of gas that is extremely hot. Solar energy needs 8 minutes and 20 seconds to travel 1.5 x 1011 meters from the Earth to the surface. At a temperature of 5,762 K, the sun can be seen as a black body from the perspective of thermal radiation. It has been calculated that the temperature in the sun's center zone ranges from 8 x 106 to 40 x 106 K [1].

It radiates outside the earth's atmosphere at a constant intensity and comparable black body temperature. The solar constant is the irradiance on a surface that is perpendicular to the direction of solar energy propagation at an average distance between the earth and the sun outside the atmosphere (Gsc). In order to analyze solar radiation, this constant is necessary. Therefore, a number of authors have tried to determine its precise value for use in solar engineering and science [2-9]. While Frohlich, who was referenced by Duffie and Beckman [11], supported a value of 1373 Wm^{-2}. The World Radiation Centre (WRC) accepted a value of 1367 Wm^{-2}, contrary to Darula's recommendation of 1366.1 Wm^2 as a more accurate value of Gsc [10].

Therefore, in this experiment, the irradiance on an angled glass cover is computed using the WRC value of Gsc. Only direct radiation is present in space outside of the earth's atmosphere. Solar radiation, however, experiences transmission, absorption, and scattering

as it travels through the atmosphere. The diffuse portion of the sun's energy is created through scattering [11].
As a result, both radiation and diffuse components of the solar energy reach the earth's surface. When incident on a surface, the two components of solar radiation exhibit various optical characteristics [12]. Direct beam radiation from the sun's disc reaches a receiver surface; its beams can be traced from the sun's location and are used to calculate solar angles. Additionally, according to ISO (1994), [13], the efficiency of the majority of solar collectors diminishes as diffuse irradiance increases. The solar constant alone is insufficient to adequately define the ground-based solar energy resource. The power absorbed by a collector placed at ground level is, in fact, typically severely reduced by a variety of factors and conditions. The following factors are some of the primary ones [14]:

- The field of collectors' location, particularly its latitude, determines the sun's apparent motion and, thus, its orientation. This also affects how long a solar day is.
- The atmosphere is an area of complex energy exchanges. It is characterized by a thick layer of air, which absorbs some visible radiation, aerosols and dust, which absorb and refract radiation, and clouds, which also absorb radiation.

The fundamental tenet of solar thermal energy conversion is the creation of heat from short-wave solar radiation. The term "photo-thermal conversion" can also be used to describe this energy conversion process. A portion of the radiation gets absorbed when it strikes a substance. The term "absorbing capacity" or "absorption" refers to a body's ability to absorb radiation. The power emitted by a body is represented by the emission. Kirchhoff's law establishes the connection between absorption and the power emitted by a body is represented by the emission. The relationship between absorption and emission is described by Kirchhoff's law. All bodies have a ratio of specific radiation to absorption coefficient that is constant at a given temperature and equal to the black body's specific radiation in terms of quantity. This ratio is only a function of wavelength and temperature. Within a specific wave range, matter with a high absorption capacity also exhibits a high emission capacity. Along with absorption and emission, reflection and transmission are important as well. The proportion of the reflected to incident radiation is known as the reflection coefficient. The ratio of radiation transmitted via a specific medium to the entire radioactive incident is defined by the transmission coefficient [15-20].

A vast, modular array of single-axis-tracking parabolic trough solar collectors makes up a parabolic trough solar field. These solar collectors are arranged across the sun field in numerous parallel rows, typically aligned along a horizontal north-south axis. Each solar collector assembly is a parabolic trough solar collector capable of autonomously tracking and made up of the important subsystems listed below:

1. Concentrator structure
2. Mirrors or reflectors
3. Linear receiver or heat collection element
4. Collector balance of system

The current work discusses solar concentrators that use parabolic trough collectors. The formula $Z=X^2/4f$ describes the parabolic curvature of this type of concentrator's cylindrical shape. The focal point of the parabola is indicated by the distance f, which is basically the

separation of the parabola's focal line from its vertex. Reflector material is used to cover the parabola's trough-shaped region in order to focus solar radiation on the focal line. To do this, the parabola's optical axis (symmetry plane) must face the sun's incoming light. To put it another way, for such systems to work, they must track the sun on a single axis. Figure 1, displays a parabolic trough collector and shows how the sunlight's direct beam component reflects back to the receiver at the parabolic reflectors' focus. The solar collector assembly is the fundamental part of the solar field (SCA). The metal support structure; the parabolic reflectors (mirrors) that make up each SCA's independently tracking group of parabolic trough sun collectors; and the parabolic trough solar filed technology.

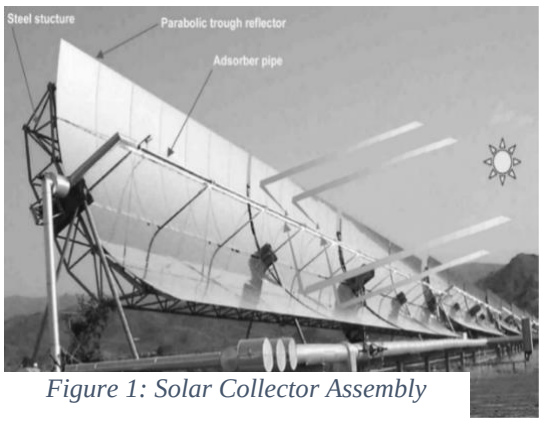

Figure 1: Solar Collector Assembly

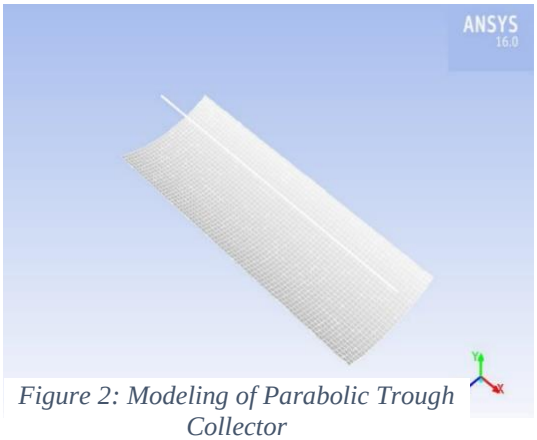

Figure 2: Modeling of Parabolic Trough Collector

2 Results and Discussions

2.1 Mesh Size

Various researchers reported numerical studies. Numerical study on a parabolic trough collector based on Fluent to predict the performance of the collector. The study determined distribute the temperature in the tube and in the four seasons of year, as show in figure 2. Modeling of parabolic trough.

The 3D structured mesh of PTC in present work was designed using point wise program. The number of mesh size was selected after performing a mesh size independence test. The mesh size independence test acts for 5 meshes with different mesh size to study the change in outlet temperature among the different meshes. The mesh size was gradually and uniformly increased from 633,017.64 cells to 945,619.84 cells. Figure 3 shows that the outlet temperature is almost constant for cells greater than 781,504 cells. Therefore, a mesh size of 781,504 cells was adopted in the present work to save the computational time while maintaining the accuracy of the results.

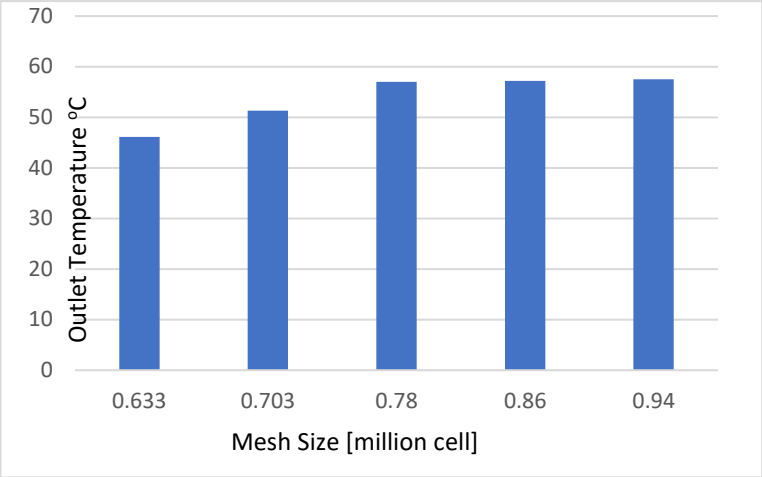

Figure 3: Mesh Size [million cell]

2.2 First Season (winter)

Experiments were done during winter starting from January 15 to January 21. On the first day, the initial temperature entered to the parabolic trough collector (PTC) was 19 ^{0}C, according to the temperature that day at that time.
Then for next days, the final temperature reached on a certain day was used as the initial temperature for the following day, taking in to consideration the percentage error cause due to the decreases in temperatures at night. After almost a week, it was noticed that the temperature in the parabolic trough collector (PTC) become constant. Results are shown in figures (5-11). Table 1 illustrates the specifications used for the heat loss using Ansys model in January.

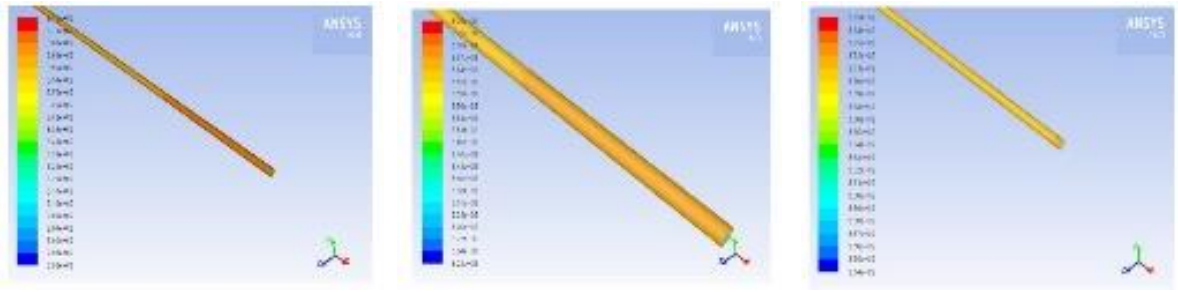

(a) (b) (c)

Figure 4: Outlet temperature variation contours in January (a) first day (b) fourth day (c) last day

Figure 4 shows the temperature distributed inside the pipe at mass flow rate 1.41 kg/s, which is the actual mass flow rate of the used oil. It was inspected that the temperature increases more in the pipe with lower mass flow rate. For example, when the initial temperature was 19 ^{0}C and the mass flow rate was 1.41 kg/s, the final temperature was 32^{0}C. However using the same temperature with mass flow rates 0.8 and 2 Kg/s, the final temperatures reached were 37 ^{0}C and 24 ^{0}C respectively.

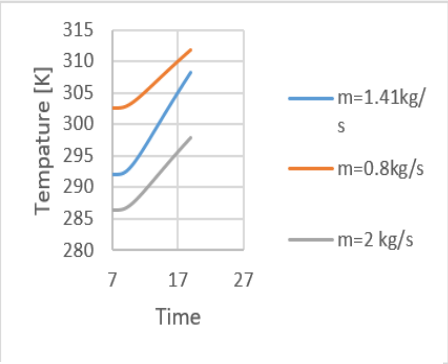

Figure 5: Outlet Temperature variation along tube on 15th January

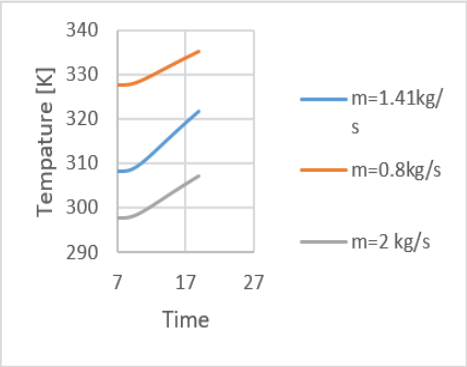

Figure 6: Outlet Temperature variation along tube on 16th January

Table 1: Specifications used for the heat loss using Ansys model in January

Parameter	Value
Inlet temperature (K)	292, 353
Beam radiation (W/m2)	737, 742, 727, 732, 626 , 731 , 632
Atmospheric air pressure	1 atm
Heat transfer fluid	VP-1
Heat transfer fluid flow rate	1.41(kg/s)

2.3 Second Season (spring)

Just like the first month, during April output temperatures were also measured using different mass flow rates. However due to the rise in temperature, the input temperature used was 30^0c. As a result the heating process in April took less time than the heating process in January. Measurements of the output temperatures are shown in figures (12-17). Figures (18) and (19) are used to ensure that equilibrium was reached. Table 2 illustrates the specifications used for the heat loss using Ansys model in April.

2.4 Third Season (summer)

Summer is the warmest season of the year, that's why studying the distribution of temperature in the parabolic trough collector (PTC) during July took only three days, from July 15th to July 17th. At the end of first day, temperature reached 380K with mass flow rate 1.41kg/s.

The input temperature of the second day was higher than the first day, although the heat losses were taken in to consideration. Measurements were taken for a third day to make sure that temperature reached equilibrium which is boiling point of the oil used. Results are shown in figures (20-22). Table 3 illustrates the specifications used for the heat loss using Ansys model in July.

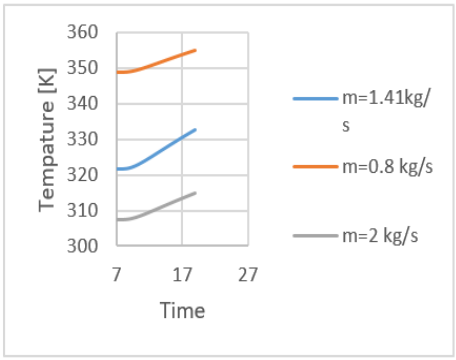

Figure 7: Outlet Temperature variation along tube on 17th January

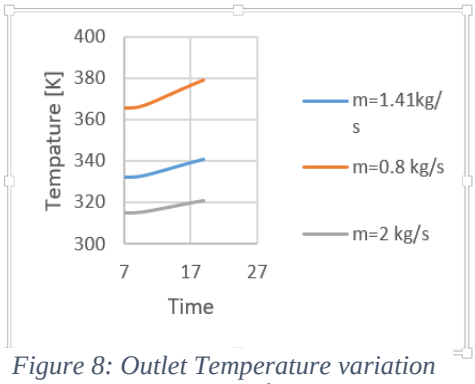

Figure 8: Outlet Temperature variation along tube on 18th January

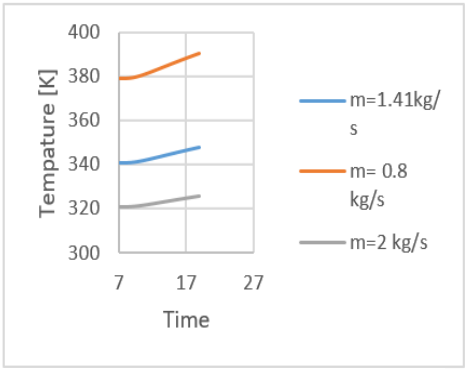

Figure 9: Outlet Temperature variation along tube on 19th January

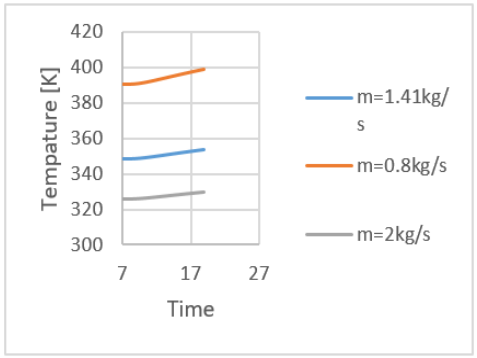

Figure 10: Outlet Temperature variation along tube on 20th January

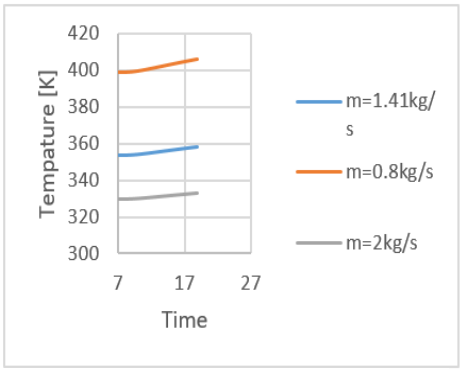

Figure 11: Outlet Temperature variation along tube on 21st January

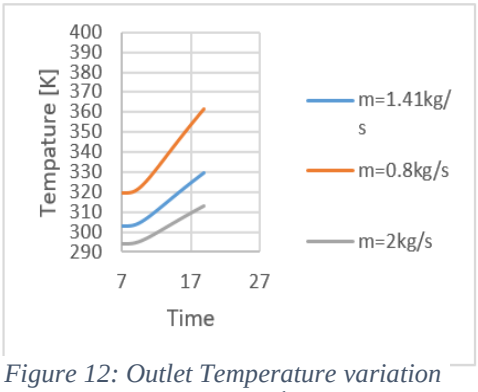

Figure 12: Outlet Temperature variation along tube on 15th April

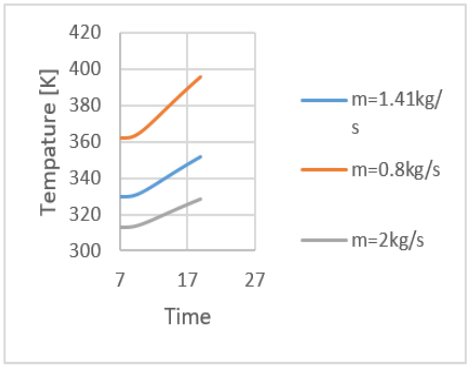

Figure 13: Outlet Temperature variation along tube on 16th April

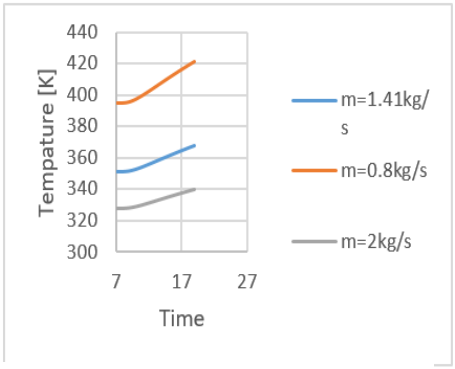

Figure 14: Outlet Temperature variation along tube on 17th April

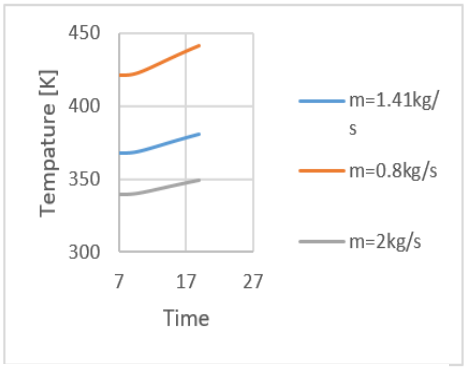

Figure 15: Outlet Temperature variation along tube on 18th April

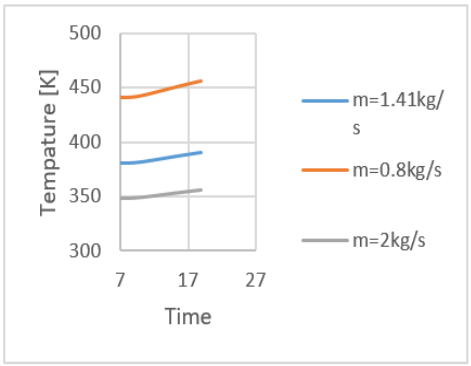

Figure 16: Outlet Temperature variation along tube on 19th April

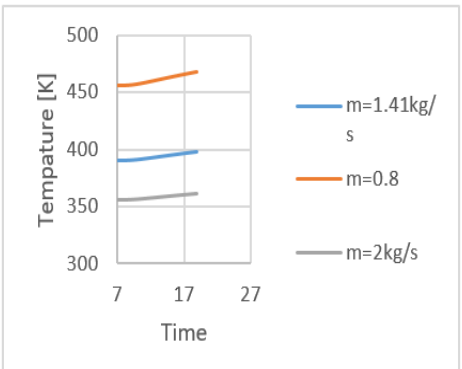

Figure 17: Outlet Temperature variation along tube on 20th April

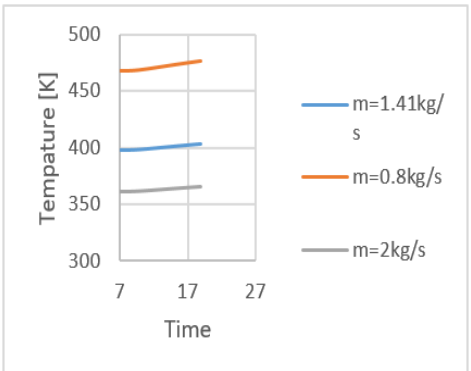

Figure 18: Outlet Temperature variation along tube on 21st April

Table 2: Specifications used for the heat loss using Ansys model in April

Parameter	Value
Inlet temperature (K)	303, 403
Beam radiation (W/m^2)	736, 742, 721, 727, 703 , 698 , 656, 742
Atmospheric air pressure	1 atm
Heat transfer fluid	VP-1
Heat transfer fluid flow rate	1.41(kg/s)

Table 3: Specifications used for the heat loss using Ansys model in July

Parameter	Value
Inlet temperature (K)	310, 425
Beam radiation (W/m2)	626, 593, 627
Atmospheric air pressure	1 atm
Heat transfer fluid	VP-1
Heat transfer fluid flow rate	1.41(kg/s)

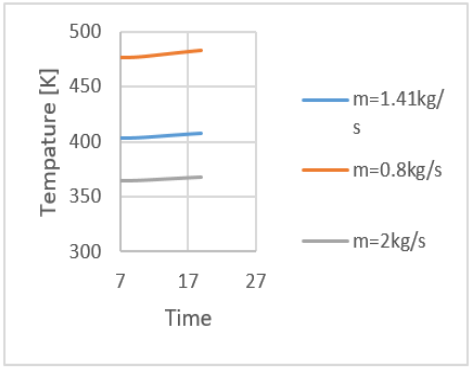

Figure 20: Outlet Temperature variation along tube on 22nd April

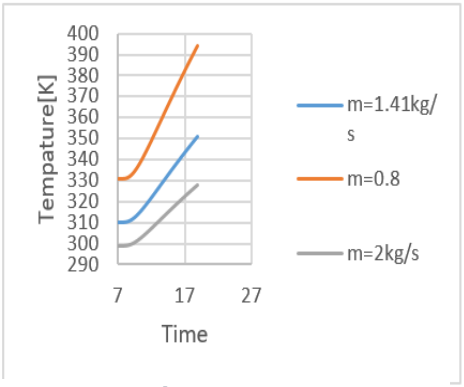

Figure 19: Outlet Temperature variation along tube on 15th July

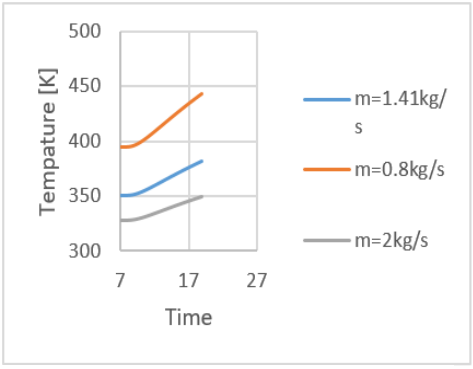

Figure 21: Outlet Temperature variation along tube on 16th July

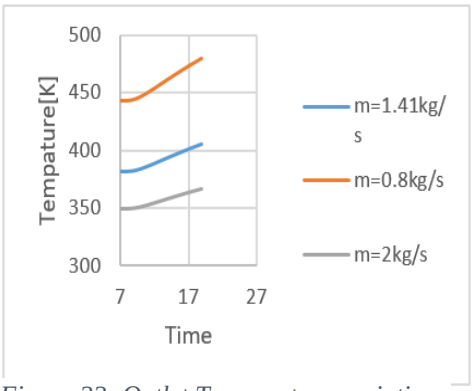

Figure 22: Outlet Temperature variation along tube on 17th July

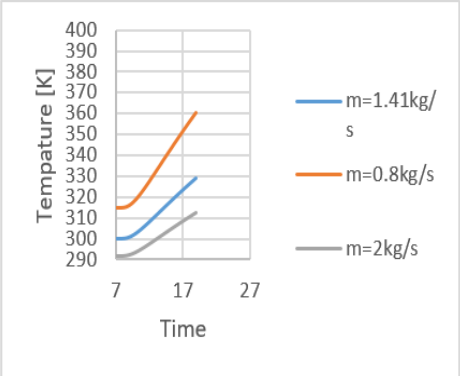

Figure 23: Outlet Temperature variation along tube on 15th October

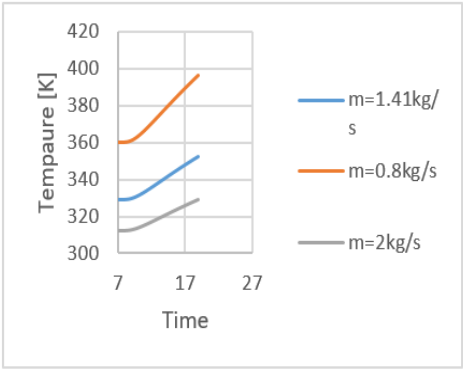

Figure 24: Outlet Temperature variation along tube on 16th October

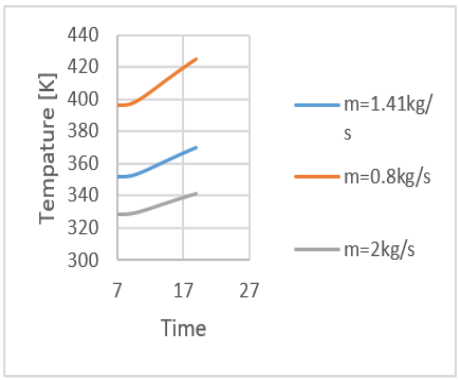

Figure 25: Outlet Temperature variation along tube on 17th October

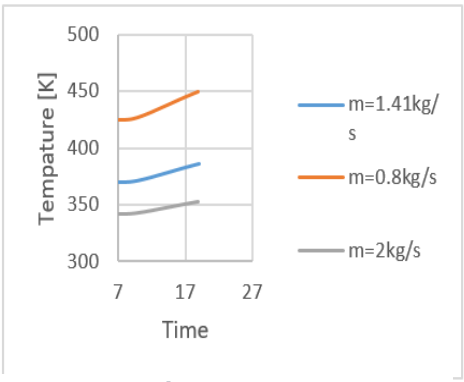

Figure 26: Outlet Temperature variation along tube on 18th October

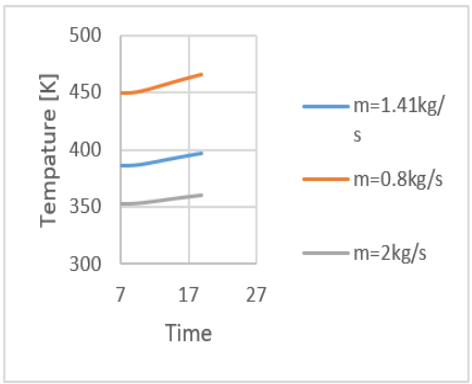

Figure 27: Outlet Temperature variation along tube on 19th October

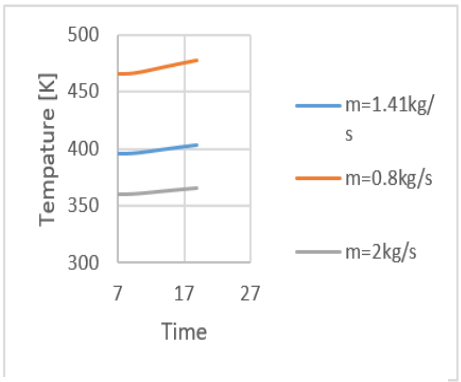

Figure 28: Outlet Temperature variation along tube on 20th October

Table 4: Specifications used for the heat loss using Ansys model in October

Parameter	Value
Inlet temperature (K)	300, 403
Beam radiation (W/m^2)	541, 530, 534, 532, 509, 508, 466
Atmospheric air pressure	1 atm
Heat transfer fluid	VP-1
Heat transfer fluid flow rate	1.41(kg/s)

2.5 Fourth Season (fall)

The winds tend to be stronger and temperatures lower during summer. As a result, the starting heating temperature. In October was 300K unlike July in which it was 310K. The temperature increased from 300K to 328K on the first day. It continued to increase for the following five days, then reached thermal equilibrium on the sixth day as shown in figures (23-28). Table 4 illustrates the specifications used for the heat loss using Ansys model in October.

3 Conclusion

Numerous academics presented numerical studies in this article. Fluent was used to forecast the collector's performance based on numerical analysis of a parabolic trough collector. The study found how to distribute the tube's temperature throughout the four distinct seasons. In the current work, a point-wise software was used to build the 3D structured mesh of PTC. The major parameters such as optical efficiency, heat transfer coefficient of working fluid, heat flux, reflection, transmission, adsorption, diameter of absorber, length of collector, etc. should be optimised to withstand environmental conditions, according to the structural and optical performance analysis on PTC.

4 References

[1] Aly, N.H., Karameldin, A. and Shamloul, M.M., 1999. Modelling and simulation of steam jet ejectors. desalination, 123(1), pp.1-8.

[2] Quaschning, V., Kistner, R. and Ortmanns, W., 2002. Influence of direct normal irradiance variation on the optimal parabolic trough field size: A problem solved with technical and economical simulations. J. Sol. Energy Eng., 124(2), pp.160-164.

[3] Lüpfert, E., Pottler, K., Ulmer, S., Riffelmann, K.J., Neumann, A. and Schiricke, B., 2007. Parabolic trough optical performance analysis techniques.

[4] Yang, Y., Cui, Y., Hou, H., Guo, X., Yang, Z. and Wang, N., 2008. Research on solar aided coal-fired power generation system and performance analysis. Science in China Series E: Technological Sciences, 51(8), pp.1211-1221.

[5] Jin, H., Hong, H., Sui, J. and Liu, Q., 2009. Fundamental study of novel mid-and low-temperature solar thermochemical energy conversion. Science in China Series E: Technological Sciences, 52(5), pp.1135-1152.
[6] Odeh, S.D., Morrison, G.L. and Behnia, M., 1998. Modelling of parabolic trough direct steam generation solar collectors. Solar energy, 62(6), pp.395-406.
[7] Liu, Q., Wang, Y., Gao, Z., Sui, J., Jin, H. and Li, H., 2010. Experimental investigation on a parabolic trough solar collector for thermal power generation. Science in China Series E: Technological Sciences, 53(1), pp.52-56.
[8] Senthilkumar, S., Perumal, K. and Srinivasan, P.S.S., 2009. Optical and thermal performance of a three-dimensional compound parabolic concentrator for spherical absorber. Sadhana, 34(3), pp.369-380.
[9] Lüpfert, E., Riffelmann, K.J., Price, H., Burkholder, F. and Moss, T., 2008. Experimental analysis of overall thermal properties of parabolic trough receivers. Journal of solar energy engineering, 130(2).
[10] Steinmann, W.D., Eck, M. and Laing, D., 2005. Solarthermal parabolic trough power plants with integrated storage capacity. International journal of energy technology and policy, 3(1-2), pp.123-336.
[11] Duffie and Beckman, "Solar Engineering of Thermal processes", Second edition, New York, A Wily-Interscience Publication, 2006.
[12] Wagner, M. and Gilman, P., 2011. System Advisor Model Documentation Technical Manual for the Physical Trough Model. National Renewable Energy Laboratory, Mar., Golden, CO.
[13] Roesle, M., Coskun, V. and Steinfeld, A., 2011. Numerical analysis of heat loss from a parabolic trough absorber tube with active vacuum system. Journal of Solar Energy Engineering, 133(3).
[14] Duffie and W. Beckman, "solar engineering of thermal processes", Madison, Wisconsin, 1980.
[15] Spiegler K., and Laird A., “Principles of Desalination – Part A”, Book, Academic Press, 1980.
[16] Krishna, Y., Faizal, M., Saidur, R., Ng, K.C. and Aslfattahi, N., 2020. State-of-the-art heat transfer fluids for parabolic trough collector. International Journal of Heat and Mass Transfer, 152, p.119541.
[17] Abed, N. and Afgan, I., 2020. An extensive review of various technologies for enhancing the thermal and optical performances of parabolic trough collectors. International Journal of Energy Research, 44(7), pp.5117-5164.
[18] Tiwari, A.K., Kumar, V., Said, Z. and Paliwal, H.K., 2021. A review on the application of hybrid nanofluids for parabolic trough collector: Recent progress and outlook. Journal of Cleaner Production, 292, p.126031.
[19] El Kouche, A. and Gallego, F.O., 2022. Modeling and numerical simulation of a parabolic trough collector using an HTF with temperature dependent physical properties. *Mathematics and Computers in Simulation*, *192*, pp.430-451.
[20] Qu, J., Zhou, G., Zhang, M., Shang, L. and Yu, W., 2023. Effect of reverse irradiation angle on the photo-thermal conversion performance of MXene nanofluid-based direct absorption solar collector. Solar Energy Materials and Solar Cells, 251, p.112164.